Meteorological Effects on Long-Range Outdoor Sound Propagation

Helmut Klug

University of Oldenburg, P.O.B. 2503, FB 8
D-2900 Oldenburg, FRG

N91-16696

I. INTRODUCTION

Measurements of sound propagation over distances up to 1000 m were carried out with an impulse sound source offering reproducible, short time signals. Temperature and wind speed at several heights were monitored simultaneously; the meteorological data are used to determine the sound speed gradients according to the Monin-Obukhov similarity theory. The sound speed profile is compared to a corresponding prediction, gained through the measured travel time difference between direct and ground reflected pulse (which depends on the sound speed gradient). Positive sound speed gradients cause bending of the sound rays towards the ground yielding enhanced sound pressure levels. The measured meteorological effects on sound propagation are discussed and illustrated by ray tracing methods.

II. SOUND SPEED PROFILES

Wind speed and temperature are functions of elevation above ground. They are interrelated and can be described by the Monin-Obukhov similarity theory /1/ using two parameters, the friction velocity u_* and the scaling temperature T_*. The Monin-Obukhov Length L is a stability parameter for the turbulent atmospheric surface layer:

$$L = (T_m/gk)(u_*^2/T_*)$$

T_m: representative temperature, g: acceleration due to gravity, k: von Kármáns constant (0.41).

The sound speed profile can be described by

$$c(z) = c(z_0) + a'(ln(z/z_0) + \psi(z/L)) \tag{1}$$

where $a' = u_*/k + 0.6T_*/k$ and z_0 is the roughness length.

For the stable case (positive temperature gradient, strongest bending of sound rays towards the ground), $\psi(z/L) = 5z/L$, and the sound speed gradient is:

$$dc/dz = (a'/z)(1+5z/L) \tag{2}$$

Examples of measured temperature and wind speed profiles are shown in Fig. 1. The parameters u_* and T_* are calculated from those measured data by least square methods /2/. In the unstable case wind speed and temperature almost remain constant in larger elevations (no sound speed gradient), while in the stable case there is still an increase in wind speed and temperature. Close to the ground the profiles are 'logarithmic' in both cases.

155

III. ACOUSTICALLY MEASURED SOUND SPEED GRADIENTS

Measured travel time differences between direct and ground reflected sound can be used to estimate the sound speed profile during the measurement. The geometrical time difference Δt_g is:

$$\Delta t_g = \Delta D/c = [\sqrt{(h_s + h_r)^2 + D^2} - \sqrt{(h_s - h_r)^2 + D^2}]/c \qquad (3)$$

c: sound speed ; h_s: source height; h_r: receiver height.

The sound speed profile c(z) causes an additional time difference $\Delta t'$, the total time difference Δt between direct and ground reflected sound is:

$$\Delta t = \Delta t' + \Delta t_g \qquad (4)$$

For small deviations of the actually curved ray path from the geometrical path the travel time of the ground reflected pulse can be estimated to be for the stable case /3/:

$$T_{refl} = \int c(z)^{-1} ds = Dc(z_0)^{-2} [c(z_0) - a' ln(z'/z_0) + a' - 2.5a'z'/L] + \Delta t_g \qquad (5)$$

where $z' = h_s = h_r$. The travel time of the direct pulse at height z' is:

$$T_{dir} = D/c(z') = D/[c(z_0) + a' ln(z'/z_0) + 5a'z'/L]$$

$$= Dc(z_0)^{-2}[c(z_0) - a ln(z'/z_0) - 5a'z'/L] \qquad (6)$$

and the travel time difference is:

$$\Delta t = T_{refl} - T_{dir} = [a'(1 + 2.5z'/L)]D/c(z_0)^2 + \Delta t_g. \qquad (7)$$

Two measurements of the travel time difference at different heights z' are necessary to determine the parameters a' and L.

Close to the ground or for the nearly neutral case (z/L becomes 0) the sound speed profile becomes 'logarithmic',

$$c(z) = c(z_0) + a ln(z/z_0) \quad \text{and} \quad dc/dz = a/z, \qquad (8)$$

the parameter a can be calculated from the measured time difference for only one source-receiver height:

$$a = \Delta t' c(z_0)^2/D \qquad (9)$$

IV. SOUND PROPAGATION MEASUREMENTS

The impulse sound source /4/ used for the acoustical measurements consists of a capacitor (100 μF, 3.5 kV), which is discharged over a spark gap. A reproducible short pulse (less than 1 ms) is radiated spherically (sound pressure level 150 dB at 1 m distance). As an example Fig. 2 shows a measured time signal close to the sound source. The time delay between direct and ground reflected pulse (here 8 ms) is mainly caused by geometry. A reference signal monitored in an unechoic room at 6.25 m distance to the sound source is used to calculate the SPL re free field for each frequency.

Two examples of downwind sound propagation measurements (8 August 1988 and 3 November 1988) are shown in the following. Measurements for several geometries done in the afternoon (unstable conditions) were repeated a few hours later under stable conditions (positive temperature gradient). The resulting meteorological effects are discussed.

August-measurement

For a distance of 250 m the measured time signal is shown in Fig. 3 a (temperature and wind speed profile see Fig. 1 c). The travel time difference Δt_g resulting from geometry is 3.7 ms. The measured time difference Δt (determined from the magnitude of the autocorrelation function of the measured sound pressure signal) is 5.3 ms (see Fig. 3b), the additional time delay $\Delta t' = 1.6$ ms being due to meteorological effects (wind speed and temperature). It can be used (eq. 8,9) to calculate the sound speed gradient:

$$a = \Delta t' c(z_0)^2/D = 0.7 \text{ m/s}; \quad dc/dz = a/z = 0.7 \text{ 1/s}$$

A few hours earlier (meteorological conditions see Fig. 1 b) a time difference $\Delta t = 4.6$ ms was measured for the same geometry, yielding a parameter $a = 0.4$ m/s.

For a source and receiver height of 12.5 m there is only a small change in the measured SPL due to meteorological effects (Fig. 4 a). The interference pattern is shifted a little towards lower frequencies for the evening measurement, the sound pressure level increasing about 1 dB. For source and receiver situated closer to the ground (2 m, Fig. 4 b) the different meteorological conditions yield an evident shift of the 'ground dip' to lower frequencies. For a distance of 1000 m (h_s: 12.5 m and 5 m; h_r: 5 m, Fig. 5) no 'ground dip' occurs in the measured frequency range.

November-measurement

Fig. 6 a-d show SPL's for different geometries and two meteorological conditions. For $h_s = h_r = 5$ m and 100 m distance (SPL see fig. 6 a) a time difference $\Delta t = 1.7$ ms was measured at 13.40, increasing to $\Delta t = 2$ ms two hours later (wind speed about 2 m/s in both cases, but negative temperature gradient in the first and positive temperature gradient in the second case). The time difference Δt_g due to geometry is 1.5 ms, $\Delta t'$ increases from 0.2 ms to 0.5 ms, the sound speed gradient in the late afternoon is more than twice as large as in the early afternoon.

The meteorological effects are strongest for low source heights and for large distances. The 'ground dip' is shifted towards lower frequencies with increasing sound speed gradient. If source and receiver are closer to the ground than in Fig. 6 a ($h_s = h_r = 1.5$ m, D = 100 m, Fig 6 b) an evident 'ground dip' around 400 Hz occurs which is reduced for the stable measurement. Fig. 6 c shows a measurement at 825 m distance ($h_s = 1.5$ m, $h_r = 5$ m). The broken line is the calculated SPL using a single-parameter impedance model (see /5/) and a flow resistivity typical for grass covered ground (no sound speed gradient assumed). The positive sound speed gradient reduces the ground dip. For the stable case

(strongest sound speed gradient) the SPL is increased some 20 dB around 500 Hz. Fig. 6 d shows the SPL for a source height of 5 m. The measured SPL is larger than that for a source height of 1.5 m.

A ray tracing simulation for the 825 m measurement under stable conditions (Fig. 6 d) is shown in Fig. 7. Multiple reflections at the ground and focussing effects (see /6/) should result in larger sound pressure levels. Indeed, the sound pressure level is increased about 10 dB for the stronger sound speed gradient. The measured time signals corresponding to the spectra in Fig. 6 d also show the expected differences (see Fig. 8). While for the 'unstable' measurement direct and ground reflected sound arrive almost at the same time, a lot of ground reflected pulses with enhanced pressure levels are observed for the 'stable' measurement yielding a signal of more than 10 ms length. Calculations with ray tracing methods /7/ for the stable meteorological condition predict a travel time difference between the direct ray (which arrives first) and the latest multiply reflected ray of 13 ms, in good agreement with the measurement.

In Fig. 9 the sound speed gradient is plotted as a function of elevation above ground. Curve (a) represents the gradient calculated from the acoustical measurement, curve (b) is a best fit to the measured wind speed and temperature values. Good agreement is achieved close to the ground where the sound speed profile has a 'logarithmic' shape. With increasing height the curves differ due to the influence of the stability (z/L is not small compared to 1 in eq. (2)).

<div align="center">V. CONCLUDING REMARKS</div>

Sound speed gradients determined from acoustical measurements represent integrated values during the actual travel time and along the actual sound path. Meteorological data in order to determine sound speed gradients, on the other hand, are measured locally and require several sensors (wind speed and temperature) of high accuracy close to the propagation area.

Downwind sound propagation (comparable wind speeds) is extremely sensitive to the stability of the atmospheric surface layer. Positive temperature gradients (stable conditions) yield a positive sound speed gradient even at large elevations, where negative temperature gradients (unstable conditions) yield a negligible sound speed gradient. Close to the ground the sound speed profile has a 'logarithmic' shape and the sound speed gradient can be described by one parameter a, which can be calculated from the measured travel time difference between direct and ground reflected sound.

The bending of sound rays towards the ground is strongest under stable conditions. The 'ground dip' is diminished and shifted to lower frequencies yielding negligible excess attenuation in the frequency range relevant for noise propagation. Focussing effects and multiple reflections lead to enhanced sound pressure levels.

/References/

/1/   *Monin, A.S.; Yaglom, A.M.:* Statistical Fluid mechanics:Mechanics of turbulence, Vol. 1, MIT Press, Cambridge, 1979.

/2/   *Nieustadt, F.:* The computation of the friction velocity u_* and the temperature scale T_* from Temperature and wind velocity profiles by least square methods, 235-246, Boundary-Layer-Meteorology 14, 1978.

/3/   *Klug, H.:* Schallimpulse als Meßsonde zur Bestimmung meteorologischer Einflüsse auf die Schallausbreitung, Dr.-Thesis, University of Oldenburg, 1990.

/4/   *Radek, U.; Klug, H., Mellert, V.:* Impulsive sound source of high intensity for outdoor sound propagation measurements, Proc. 13 [th] ICA, Vol. 2, 23 -26, Belgrad 1989.

/5/   *Attenborough, K.:* Acoustic impedance models for outdoor sound propagation. J. Sound and Vibration 99 (4), 521 -544, 1985.

/6/   *Mellert, V.; Klug, H.; Radek, U.:* Acoustic probing of meteorological and acoustical parameters in outdoor sound propagation, Proc. 13 [th] ICA, Vol. 2, 27 - 30, Belgrad 1989.

/7/   *Thompson, R. J.:* Ray theory for an inhomogeneous moving medium, JASA 51, 1675 - 1682, 1972.

Fig. 1: Measured wind speed and temperature profiles in the atmospheric surface layer (+). The solid line fits the measured values using the Monin-Obukhov similarity functions.
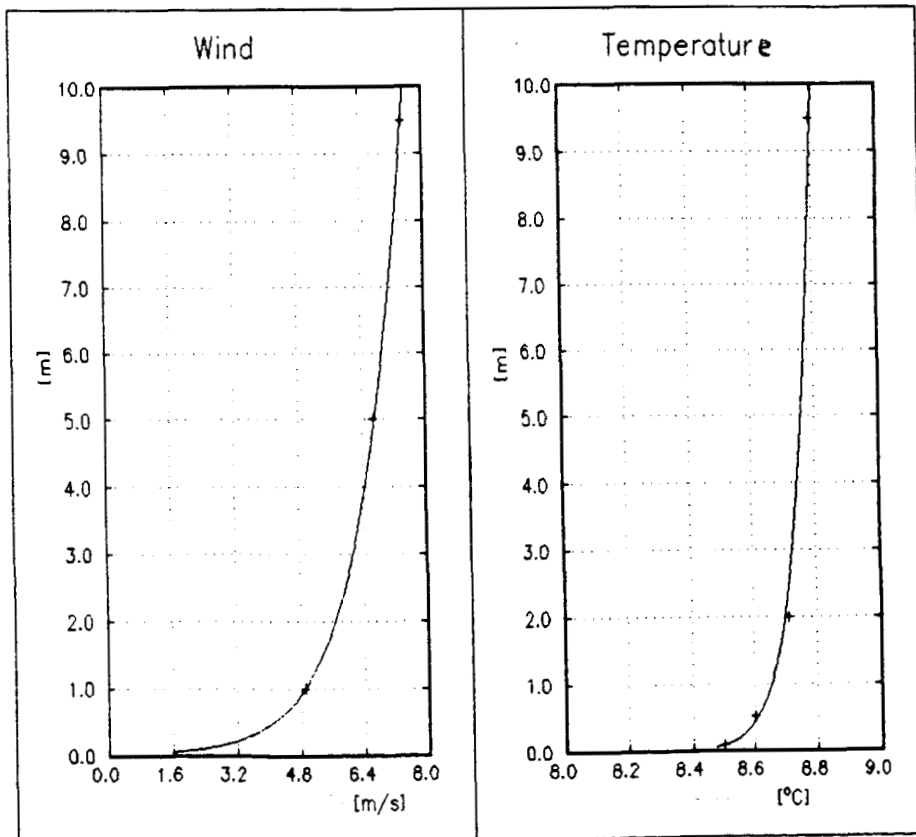
Fig. 1 a) nearly neutral (logarithmic wind profile)

24 November 1988
Time: 16.00

u_*:   *0.46 m/s*

T_*:   *+ 0.025 K*

L: *+422 m*

z_0:   *0.01 m*

Wind

Temperature

Fig. 1 b) unstable
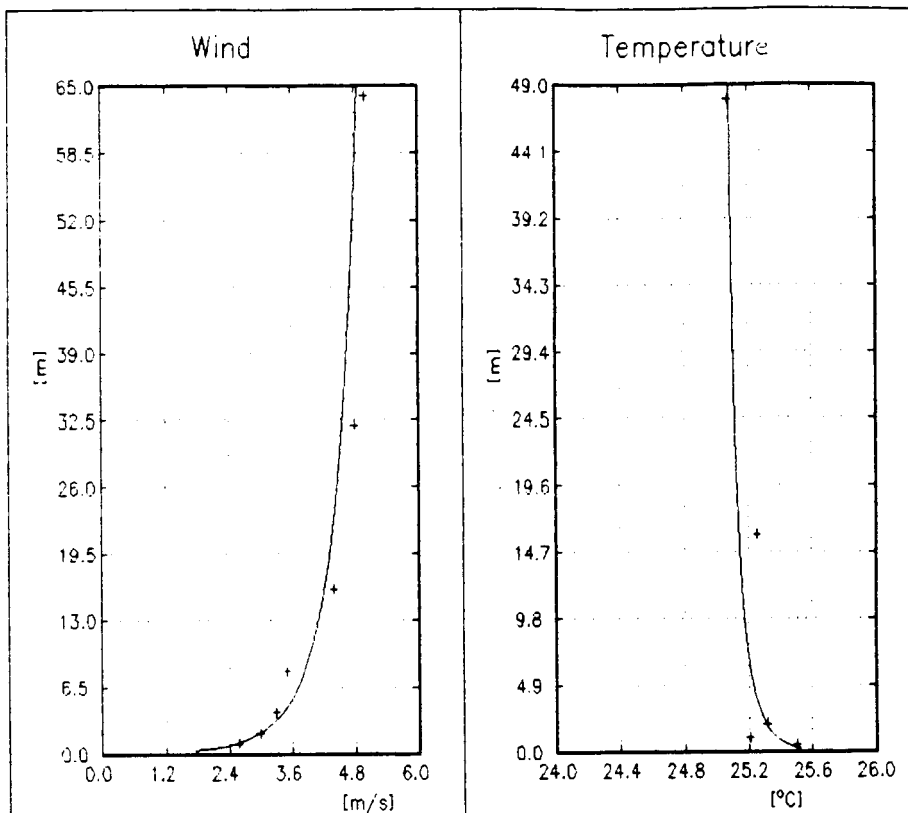
8 August 1988
Time: 16.00

u_*:	_0.28 m/s_
T_*:	_- 0.043 K_
_L:_	_- 134 m_
z_0:	_0.02 m_

Wind

Temperature
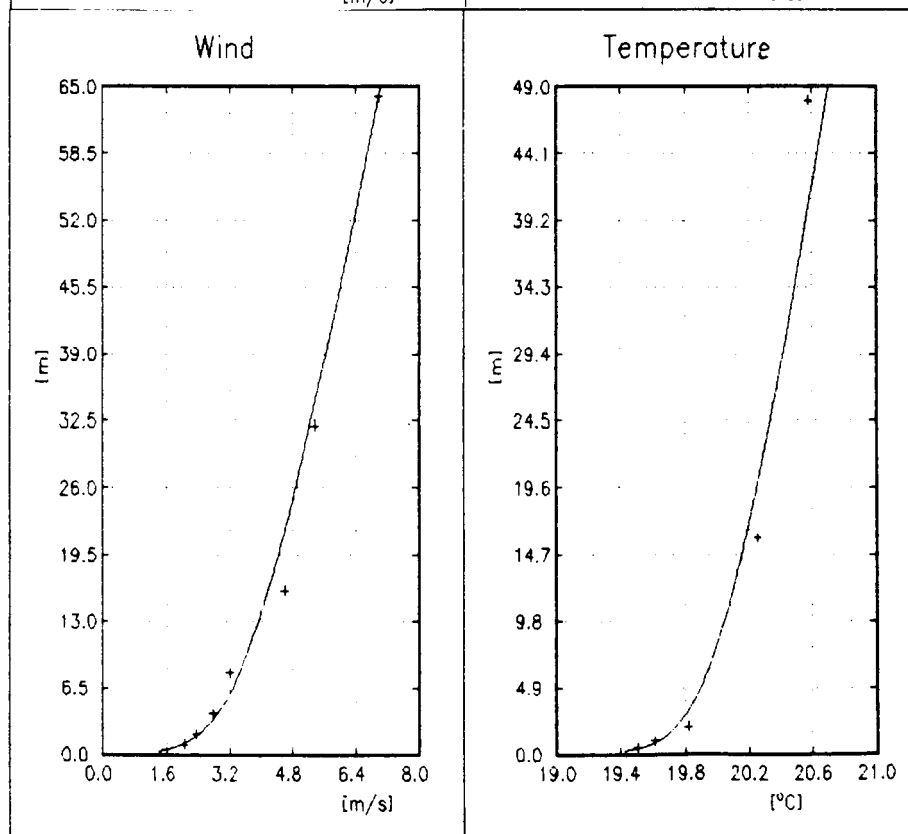
Fig. 1 c) stable

8 August 1988
Time: 21.00

u_*:	_0.22 m/s_
T_*:	_+ 0.057 K_
_L:_	_+ 63 m_
z_0:	_0.03 m_
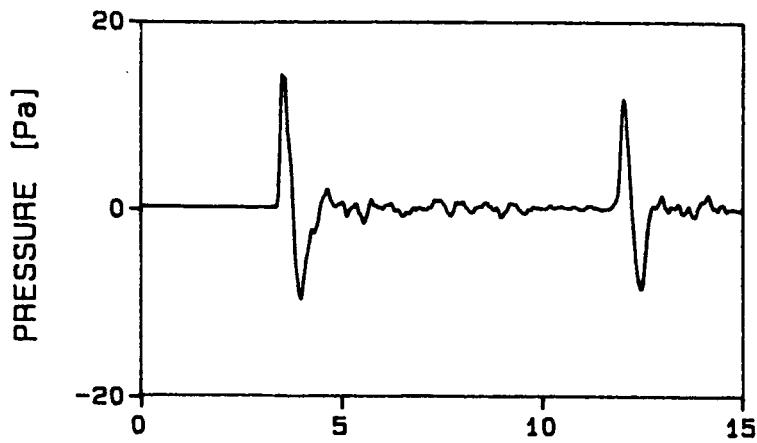
Fig. 2 : Measured time signal
$h_s = 30$ m; $h_r = 2$ m
horizontal distance: 34 m.

Fig. 3 a: Measured time signal
$h_s = h_r = 12.5$ m; distance: 250 m
(stable conditions)
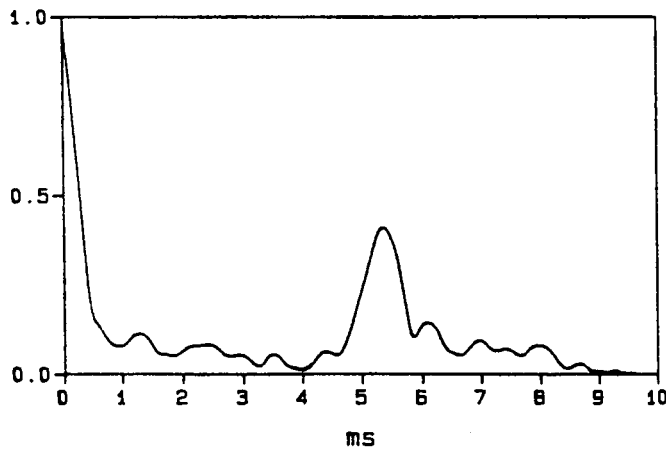
Fig. 3 b: Autocorrelation function
of the signal in a .
The maximum at 5.3 ms shows the
time difference between direct and
ground reflected pulse
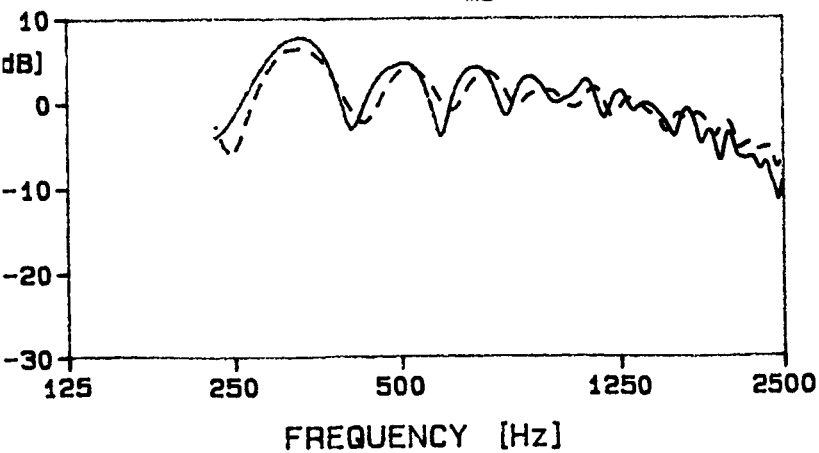
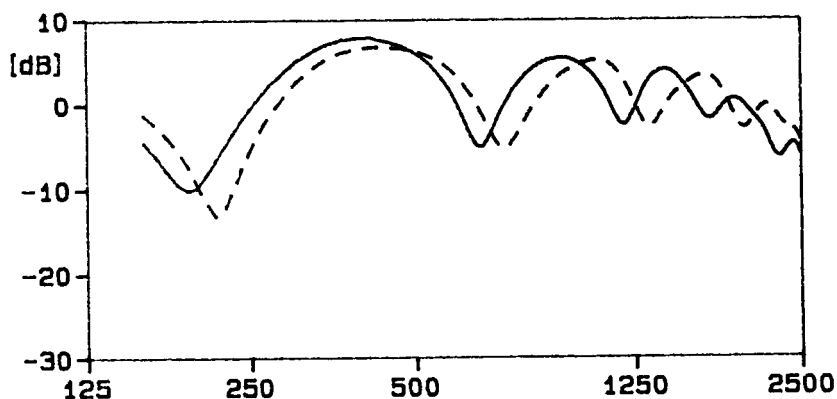*Fig.4 a:* SPL re free field
(12.5 m, 12.5 m, 250 m)
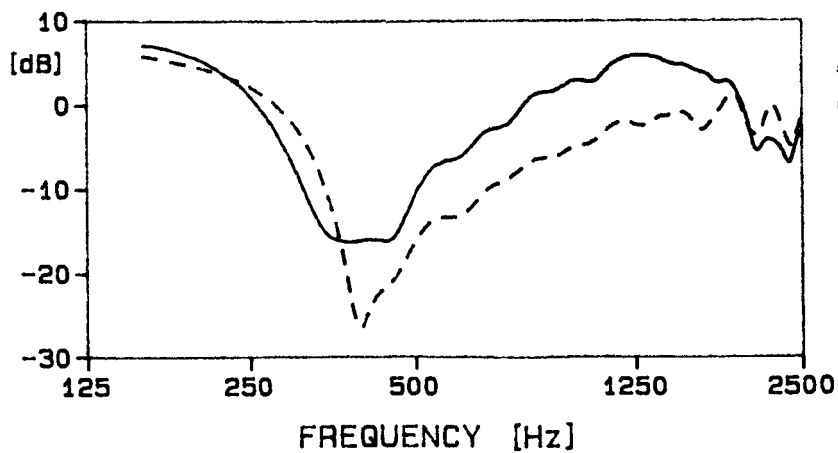———— stable conditions
– – – – unstable conditions
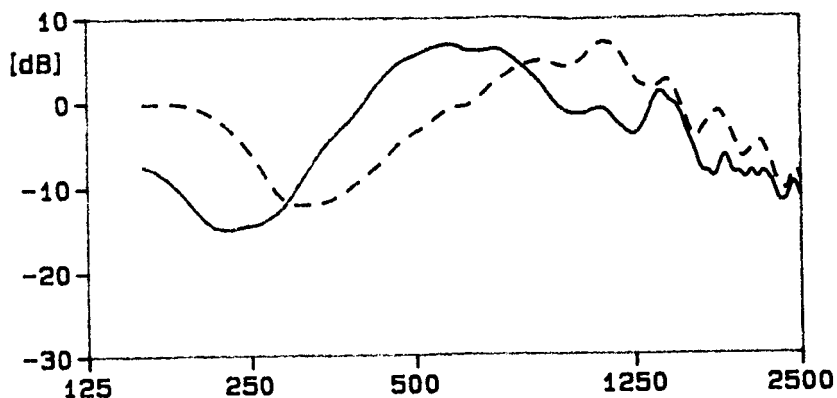
Fig. 4 b: SPL re free field
(2 m, 2 m, 250 m)
——— stable conditions
- - - - unstable conditions
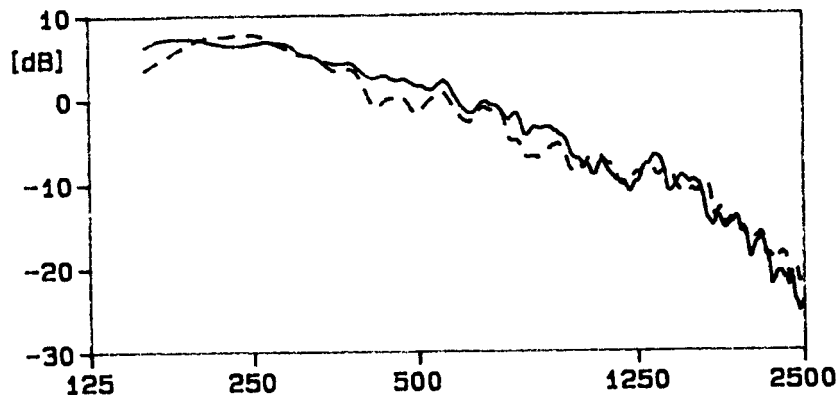
Fig. 5: SPL re free field;
——— stable conditions
(12.5 m, 5 m, 1000 m)
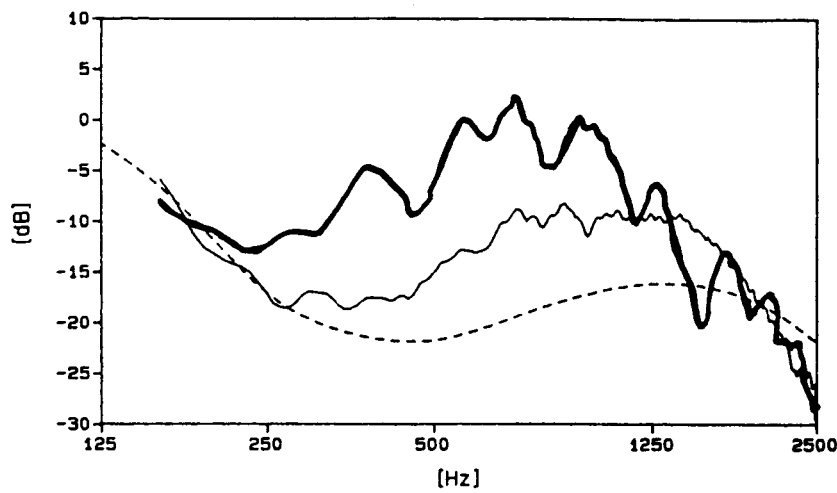- - - - - stable conditions
(5 m, 5 m, 1000 m)

Fig.6 a: SPL re free field;
(5 m, 5 m, 100 m)
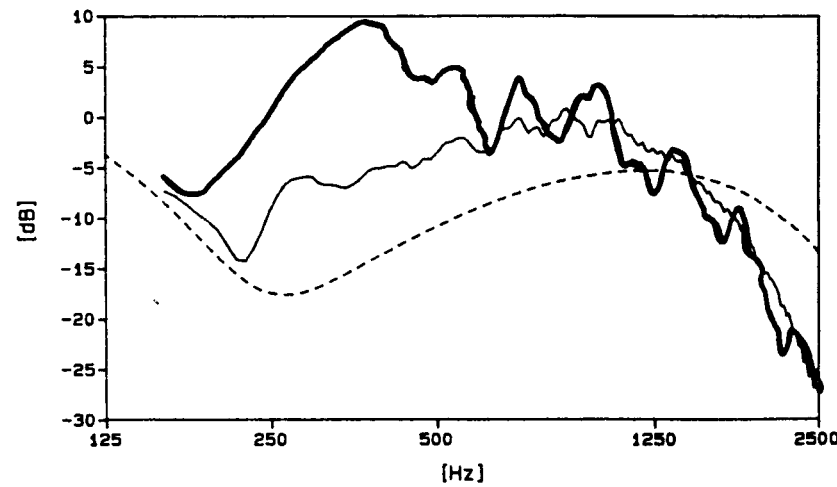——— stable conditions
- - - - unstable conditions

Fig.6 b: SPL re free field
(1.5 m, 1.5 m, 100 m)
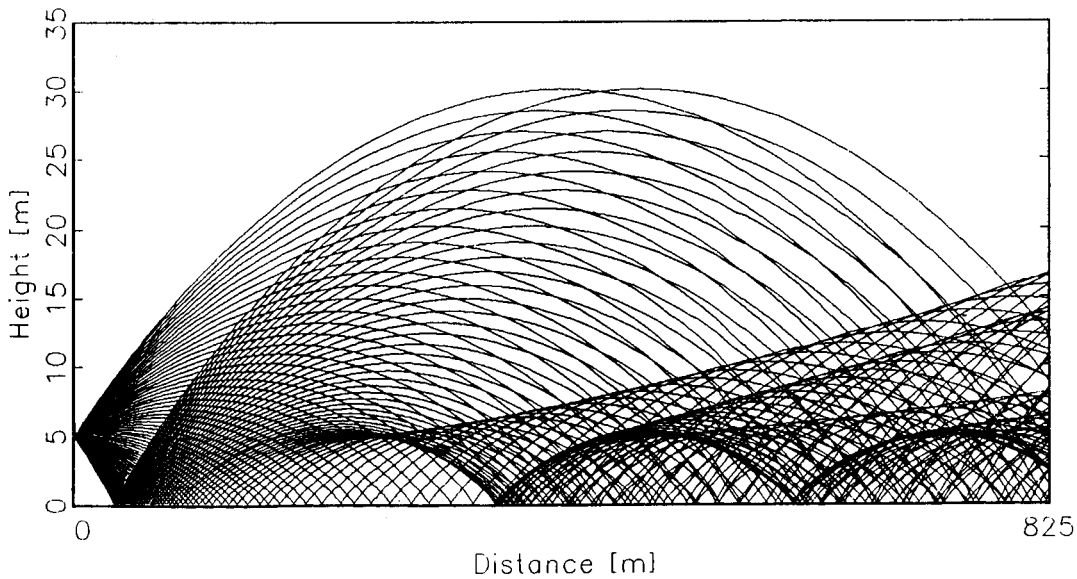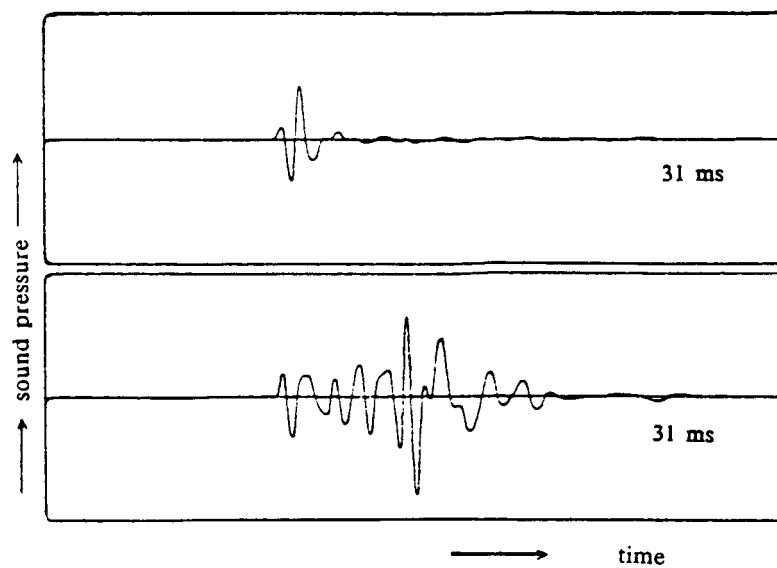——— stable conditions
- - - - unstable conditions

FREQUENCY [Hz]

162

Fig.6 c: SPL re free field
(1.5 m, 5 m, 825 m)
----- calculatet
$(\sigma = 225\ 000\ kgs^{-1}m^{-3})$
——— stable conditions
——— unstable conditions

Fig.6 d: SPL re free field
(5 m, 5 m, 825 m)
----- calculatet
$(\sigma = 225\ 000\ kgs^{-1}m^{-3})$
——— stable conditions
——— unstable conditions

Fig. 7: ray pattern plot according to measurement 6 d (stable conditions; $u_* = 0.16$, $T_* = 0.07$, $L = 28$ m, determined from measured meteorological data)

163

Fig. 8: Measured time signals
above: unstable conditions
below: stable conditions

Fig. 9: Sound speed gradient [1/s]
as a function of elevation above ground
a) measured acoustically   (Fig. 3)
b) determined by meteorological measurements
(Fig. 1 c)

164